Available online at www.sciencedirect.com

SciVerse ScienceDirect

Ceramics International 38 (2012) 2605–2608

CERAMICS INTERNATIONAL

www.elsevier.com/locate/ceramint

Short communication

Effect of K/Na ratio on piezoelectric properties of modified-$(K_{1-x}Na_x)NbO_3$ ''Hard'' lead-free piezoelectrics

Jong Bong Lim [a,*], Young-Hun Jeong [c], Myong-Ho Kim [b], Danilo Suvorov [d], Jae-Ho Jeon [a]

[a] Nano. Functional Materials Group, Korea Institute of Materials Science, Changwon, Gyeongnam 641-831, Republic of Korea
[b] School of Nano and Advanced Materials Engineering, Changwon National University, Gyeongnam 641-773, Republic of Korea
[c] Optic and Electronic Ceramics Division, Korea Institute of Ceramic Engineering & Technology, 103 Fashion Danji-gil, Geumcheon-gu, Seoul 153-801, Republic of Korea
[d] Department of Advanced Materials, Jozef Stefan Institute, Jamova 39, SI-1000 Ljubljana, Slovenia

Received 24 August 2011; received in revised form 20 October 2011; accepted 24 October 2011
Available online 29 October 2011

Abstract

0.55 mol% $K_4CuNb_8O_{23}$–$(K_{1-x}Na_x)NbO_3$ (KCN–KNNx) with $0.45 \leq x \leq 0.60$ were synthesized by conventional method. Results revealed that the increase of x was effective in changing the microstructure and relative density of KCN–KNNx. Further, varying the x resulted in a slight shift of the phase transition temperatures (T_{o-t} and T_c) toward low values. A high mechanical quality factor (Q_m) of 1850 was found at $x = 0.54$, which might be due to the build-up of an internal bias field (E_i) within KCN. Thermal hysteresis in KCN–KNNx was confirmed with x, resulting from structural changes. Thus, KCN–KNNx with $x = 0.54$ exhibits excellent piezoelectric properties with d_{33} (97 pC/N), k_p (36%), and Q_m (1850), being promising candidates for application in high-power piezoelectric devices.

Keywords: Piezoelectrics; Hard lead-free; $(K,Na)NbO_3$

1. Introduction

$Pb(Zr,Ti)O_3$ (PZT) ceramics, including PZT4 and PZT8 as ''Hard'' materials have been the mainstay of high power applications [1]. However, because of the toxicity of lead oxides, it is desirable to develop lead-free materials with comparable performances, to replace the lead-based materials [2].

Among the lead-free materials, alkali-based perovskite compounds have been studied intensively because they are environmentally friendly materials and are promising alternatives to lead-based PZT systems [3–8]. In $K_{1-x}Na_xNbO_3$, the optimum ratio of K/Na has been deemed to play an important role since Tennery and Hang [9] reported the presence of a phase boundary between two orthorhombic phases at 52.5 mol% of Na. However, this optimal K/Na ratio in $K_{1-x}Na_xNbO_3$ is still unclear. Recently, excellent piezoelectric properties were reported for $K_{1-x}Na_xNbO_3$ with an optimum K/Na ratio of 0.480/0.535 [10]. Furthermore, in our preliminary work, $0.95(K_{1-x}Na_x)NbO_3$–$0.05LiTaO_3$ system exhibited excellent piezoelectric properties at a K/Na ratio of 0.45/0.55. According to previous studies on the K/Na ratio in $K_{1-x}Na_xNbO_3$, thus a Na-rich region exhibits better piezoelectric properties than a K-rich region.

Based on previous study [11], we synthesized $(K_{1-x}Na_x)NbO_3$ with 0.55 mol% $K_4CuNb_8O_{23}$ (KCN–KNNx, $0.45 \leq x \leq 0.60$) and characterized their piezoelectric properties to confirm optimum composition with high mechanical quality factor (Q_m) for hard lead-free materials.

2. Experimental procedure

KCN–KNNx with $0.45 \leq x \leq 0.60$ were synthesized by the conventional method using high purity oxide powders (K_2CO_3, Na_2CO_3, Nb_2O_5, and CuO, 99.5%, Sigma–Aldrich, USA). KNNx and KCN were stoichiometrically weighed, mixed using ball-milling in anhydrous ethanol solution for 24 h, and calcined at 850 °C for 3 h, respectively. The calcined powders of KNNx and KCN were mixed and re-milled before pressing

* Corresponding author. Tel.: +82 10 3371 8114; fax: +82 55 280 3594.
E-mail address: limjongbong@gmail.com (J.B. Lim).

0272-8842/$36.00
doi:10.1016/j.ceramint.2011.10.065

into pellets. All samples were embedded in the source powder of the same composition to minimize the loss of alkali during sintering, and then they were sintered at 1100 °C for 2 h in a closed crucible. The sintered samples were polished parallel to 1-mm thickness and electroded with a post-fire silver paste. The density was measured by the Archimedes method. The phase purity and microstructure were examined by X-ray powder diffraction (XRD; D/MAX 2200, Rigaku, Japan) and scanning electron microscopy (FE-SEM; MIRA-II LMH, Tescan, USA). The dielectric permittivity and dielectric loss were determined using a multifrequency LCR meter (HP4294A, Agilent Technologies Ltd., Japan). High field measurements of the *P–E* hysteresis behavior were performed using a modified Sawyer–Tower circuit, driven by a high-voltage power supply (TREK Model 610).

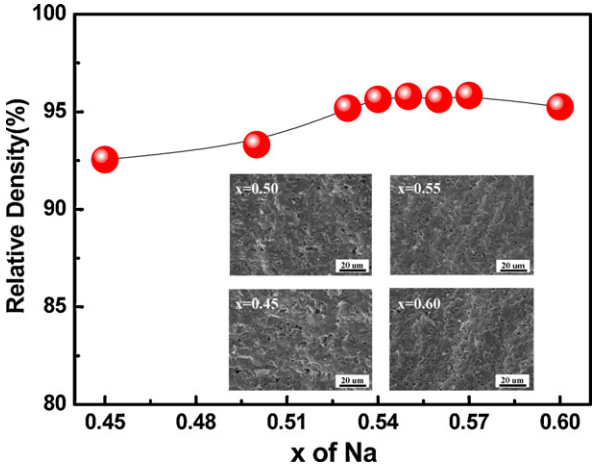

Fig. 2. Relative density and fractured surface of KCN–KNNx as a function of x.

3. Results and discussion

X-ray diffraction patterns of KCN–KNNx with $0.45 \leq x \leq 0.60$ are shown in Fig. 1(a). All the prepared samples exhibited similar diffraction patterns, representing a single orthorhombic perovskite structure. No second phase was seen over the wide composition range of $x = 0.45$–0.60 (Fig. 1(a)). Fig. 1(b) shows enlarged diffraction patterns, from 30.5° to 32.8°. The main diffraction peaks shifted slightly to higher diffraction angles with increasing x. This is readily explained by the smaller ionic radius of Na^+ (1.39 Å) as compared to that of K^+ (1.66 Å). In contrast to previous reports [11,12], the relative intensities of the main peaks for (0 0 2) and (1 1 1) remained unchanged with increasing x, indicating that no phase transition was identified by the change of K/Na ratio in this range. According to phase diagram of $KNbO_3$–$NaNbO_3$ [13], the MPB region existing two orthorhombic phases (O_1 and O_2) is very narrow. In this study, however, the changing interval of K/Na ratio in KCN–KNNx was relatively large, being in the order of 1.0 mol% near the MPB region. Therefore, it can be considered that the variation of K/Na ratio in KCN–KNNx is too large to identify the phase transition of two orthorhombic phases.

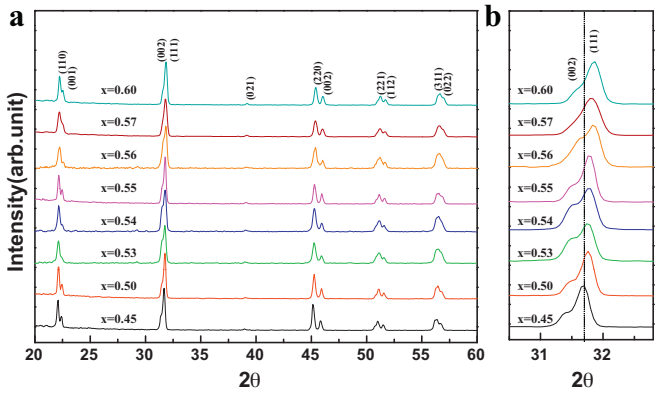

Fig. 1. X-ray diffraction patterns of: (a) KCN–KNNx with $0.45 \leq x \leq 0.60$ and (b) enlarged diffraction patterns from 30.5° to 32.8°.

Relative densities and fractured surface of KCN–KNNx are shown in Fig. 2. For $x = 0.45$, the relative density was found to be low with ~92.5%. When x was increased, the relative density increased up to 95.7% for $x = 0.55$ and then slightly decreased with a further increase in x. In the case of the fractured surface shown in the inset in Fig. 2, the sample with $x = 0.45$ exhibited a relatively porous microstructure. However, with an increase in x, the density of the microstructure increased. Despite the addition of KCN as a sintering agent, the relative densities of $x \leq 0.50$ were observed to be low with porous microstructures. According to our previous experimental data, K-rich KNNx without dopants usually shows a higher relative density than Na-rich one. This suggests that K, rather than Na, is more effective in decreasing the sintering temperature of KNNx. Thus, we can infer that when $x \leq 0.50$ in K-rich KCN–KNNx, both K and KCN formed a large amount of liquid phase during sintering, resulting in the formation of the porous microstructure, and they existed as an amorphous phase at room temperature, which caused no observation of second phase. In contrast, it can be suggested that for $x \geq 0.53$ in Na-rich KCN–KNNx, the increase in x induced a decrease in the liquid phase during sintering. Thus, the Na content can be varied to enable the optimization of the amount of liquid phase and the densification of KCN–KNNx.

The temperature dependence of the dielectric permittivity of KCN–KNNx was measured at 100 kHz during the heating cycle, as shown in Fig. 3. For $x = 0.45$, the orthorhombic–tetragonal transition temperature (T_{o-t}) was 197.7 °C and the Curie temperature (T_c) was 399.5 °C. With an increase in x, both the phase transition temperatures were found to slightly shift downward to 190.2 °C(T_{o-t}) and 394 °C (T_c) for $x = 0.6$, respectively. Thus, we can conclude that increasing x can cause the phase transition temperature to decrease. The inset in Fig. 3 shows the variation in the phase transition temperatures (T_{o-t}, T_c) through thermal hysteresis during the heating and cooling cycles, respectively. With increase in x, both T_{o-t} and T_c were found to be in thermal hysteresis, but it was not significant. In normal, the different temperature behavior at the phase transition region related to thermal hysteresis is very sensitive

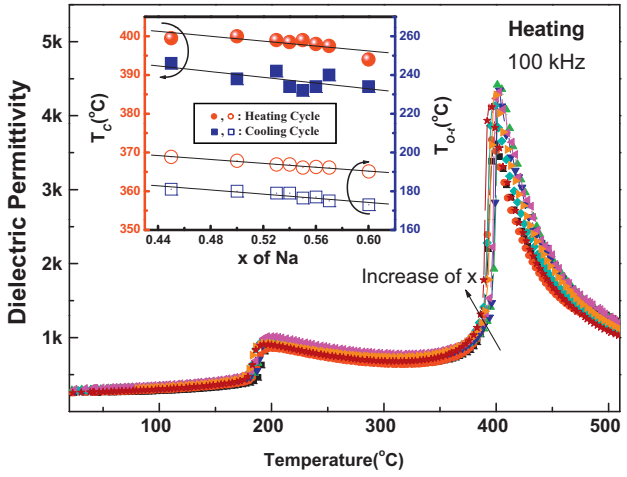

Fig. 3. Temperature dependence of the dielectric permittivity of KCN–KNNx during the heating. The inset in Fig. 3 shows the variations of T_{o-t} and T_c through the heating and cooling cycles.

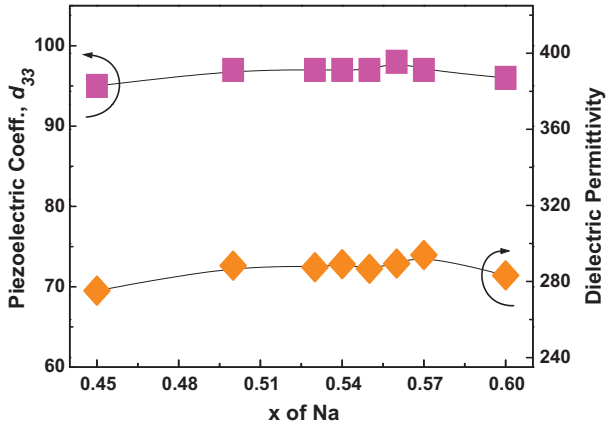

Fig. 4. Piezoelectric constant (d_{33}) and dielectric permittivity (ε_r) of KCN–KNNx as a function of x.

to the temperature ramping rate during the heating and cooling cycles. In this study, to minimize the influence of thermal fluctuation on thermal hysteresis, we have tried to control exactly both the heating and cooling rate at 1 °C/min, respectively, but we cannot exclude the possibility of temperature ramping rate effect completely, affecting to thermal hysteresis. In addition, even though Na^+ (1.39 Å) was substituted for K^+ (1.66 Å) in KCN–KNNx, attributed to a structural distortion the variation in thermal hysteresis was not significant as a function of Na content. Therefore, it can be suggested that the thermal hysteresis revealed in this system might be related to the different temperature-dependent behavior of two phases at the phase transition regions (T_{o-t}, T_c) as the first order phase transition during the heating and cooling cycles, respectively.

Fig. 4 shows the piezoelectric constant (d_{33}) and dielectric permittivity (ε_r) of KCN–KNNx as a function of x. As can be seen, with an increase in x, the d_{33} showed a small variation, with a maximum value of 98 pC/N for $x = 0.56$, whereas the ε_r increased slightly up to 294 for $x = 0.57$. However, both d_{33} and ε_r exhibited similar tendency, i.e., small variations with changes in x.

Fig. 5 shows P–E hysteresis loops of KCN–KNNx with $0.45 \leq x \leq 0.60$ as a function of the applied field and frequency. As shown in Fig. 5(a), the P–E loops exhibited a typical square shape as "Hard" lead-free materials. The remnant polarization (P_r) in the inset in Fig. 5 was plotted against x, and it was observed to increase slightly with x, but not significant. Fig. 5(b) shows the frequency dependence of the P–E hysteresis loops for $x = 0.54$ measured in the range 2–100 Hz. As the frequency was below 10 Hz, no frequency relaxation was observed, indicating nearly constant true remnant polarization and coercive field (E_c). However, increasing the frequency to 100 Hz dramatically reduced both P_r and E_c because of polarization relaxation resulting from the loss of switchable remanent polarization in the ferroelectric materials. Besides, according to the above results for frequency dependence, it can be considered that at low frequencies ($\leq$10 Hz), the KCN–KNNx system is more stable than commercial "Hard" materials such as PZT-4H [14]. This finding shows that KCN–KNNx are promising candidates for high power applications.

The mechanical quality factor (Q_m) was measured as a function of x, as shown in Fig. 6. The Q_m was found to be in the order of 820 for $x = 0.45$. As the increase of x, the Q_m increased significantly up to 1850 for $x = 0.54$, which is seven times greater than that of hot-pressed ceramics [15]. As the further increase to $x = 0.60$, the Q_m decreased to 1100. The inset in Fig. 6 shows the variations in E_c and internal bias (E_i) for the P/E loops shown in Fig. 5, respectively. Both E_c and E_i in the inset in Fig. 6 exhibited small variation, but it showed almost no dependence against x. In addition, high E_i by KCN was

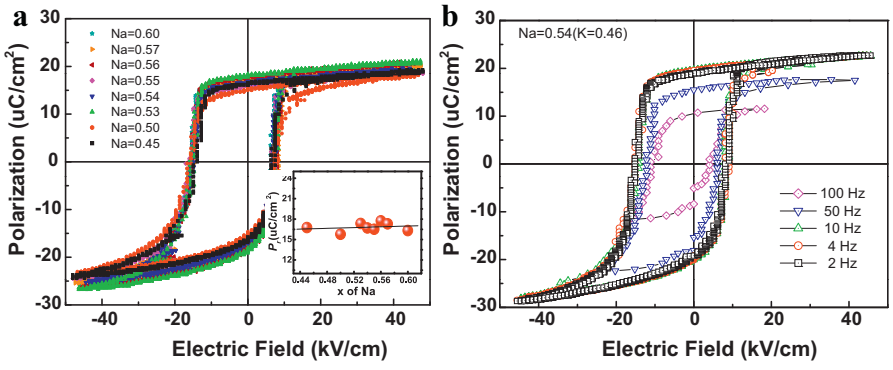

Fig. 5. P–E hysteresis loops of KCN–KNNx with $0.45 \leq x \leq 0.60$ as a function of: (a) applied fields and (b) frequencies.

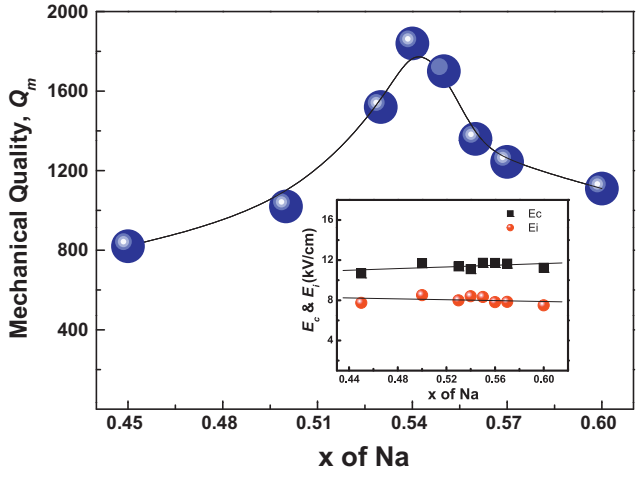

Fig. 6. Variation of mechanical quality factors (Q_m) as a function of x. The inset in Fig. 6 describes the variations of coercive field (E_c) and internal bias (E_i).

Table 1
Detailed piezoelectric properties of KCN–KNN0.54 compared to PZT8 materials.

Material	T_{o-t}/T_c (°C)	d_{33} (pC/N)	ε_{33}^T	k_p	k_t	Q_m	tan δ
KCN–KNN0.54	194/398	97	290	0.36	0.53	1850	0.003
KNN[a]	215/420	95	205	0.40	0.46	230	0.030
PZT8[a]	–/300	225	900	0.51	0.48	1000	0.004

[a] Ref. [12].

apparent in all KNNx samples, regardless of x (see the inset in Fig. 6). According to previous reports [11,16], high Q_m is affected by the formation of E_i through the acceptor and oxygen vacancy complexes. Moreover, E_i reduces hysteresis loss, especially by prohibiting domain wall motions [16]. Even though high E_i was seen for $x \leq 0.50$, the low Q_m in this study cannot be explained by the formation of E_i. In general, the Q_m is also sensitive to microstructural variations, such as those in density, liquid phase, grain size. Based on the microstructural analysis results in Fig. 2, it can be suggested that the formation of the large amount of liquid phase related to K^+ and KCN with a porous microstructure could be attributed to the reduction in the energy barrier of the defect migration and the development in a local depolarization field, which led to the observed decrease in the Q_m for KCN–KNNx with $x \leq 0.50$. This is the first report of a systematic study on the variation of Q_m with changes in the K/Na ratio for ''Hard'' lead-free KNNx. The study on the effect of K/Na ratio needs further experimental work to gain a better understanding of the ''Hard'' lead-free materials. Detailed piezoelectric properties of KCN–KNN0.54 compared to PZT8 materials are summarized in Table 1.

4. Summary

Varying x with $0.45 \leq x \leq 0.60$ in KCN–KNNx was effective in altering the microstructure, and thus the piezoelectric properties. An increase in x resulted in shifting the phase transition temperatures toward lower values and induced thermal hystersis. The Q_m was found to be high, i.e., ~1850, for KCN–KNN0.54. This result was attributed to the stabilization of the domain wall movement by the build-up of E_i. However, when $x \leq 0.50$, the Q_m was relatively low because of the formation of a large liquid phase, resulting in a porous microstructure. Thus, KCN–KNNx have the potential for high-power applications such as ultrasonic motors and transformers.

Acknowledgements

This work was financially supported by the Fundamental R&D Program for Core Technology of Materials funded by the Ministry of Knowledge Economy, Republic of Korea and by the "Gyeongnam, Changwon Science Research Park Project" of the Grant of the Korean Ministry of Education, Science and Technology.

References

[1] R.C. Pohanka, P.L. Smith, Recent advances in piezoelectric ceramics, Ch. 2, in: L.M. Levinson (Ed.), Electronic Ceramics: Properties, Devices and Applications, Marcel Dekker, New York, 1987.
[2] For example: the legislation will be enforced in the EU as the draft directives on waste from electrical and electronic equipment (WEEE), restriction of hazardous substances (RoHS) and end-of life vehicles (ELV).
[3] R. Wang, R. Xie, T. Sekiya, Y. Shimoju, Y. Akimune, H. Hirosaki, M. Ito, Piezoelectric properties of spark-plasma-sintered $(Na_{0.5}K_{0.5})NbO_3$–$PbTiO_3$ ceramics, Jpn. J. Appl. Phys. 41 (2002) 7119–7122.
[4] R.P. Wang, R.J. Xie, K. Hanada, K. Matsusaki, H. Bando, M. Itoh, Phase diagram and enhanced piezo-electricity in the strontium titanate doped potassium–sodium niobate solid solution, Phys. Status Solidi A 202 (2005) R57–R59.
[5] Y. Saito, H. Takao, T. Tani, T. Nonoyama, K. Takatori, T. Homma, T. Nagaya, M. Nakamura, Lead free piezoceramics, Nature (Lond.) 42 (2004) 84–87.
[6] Y.P. Guo, K. Kakimoto, H. Ohsato, Phase transitional behavior and piezoelectric properties of NKN–LN ceramics, Appl. Phys. Lett. 85 (2004) 4121–4123.
[7] L. Egerton, D.M. Dillon, Piezoelectric and dielectric properties of ceramics in the system potassium–sodium niobate, J. Am. Ceram. Soc. 42 (1959) 438–441.
[8] R.E. Jaeger, L. Egerton, Hot pressing of potassium–sodium niobates, J. Am. Ceram. Soc. 45 (1962) 209–213.
[9] V.J. Tennery, K.W. Hang, Thermal and X-ray diffraction studies of the $NaNbO_3$–$KNbO_3$ system, J. Appl. Phys. 39 (1968) 4749–4753.
[10] P. Zhao, B.P. Zhang, J.F. Li, High piezoelectric d_{33} coefficient in Li-modified lead-free $(Na,K)NbO_3$ ceramics sintered at optimal temperature, Appl. Phys. Lett. 90 (2007) 242909–242913.
[11] J.B. Lim, S.J. Zhang, J-.H. Jeon, T.R. Shrout, $(K,Na)NbO_3$-based ceramics for piezoelectric "Hard" lead-free materials, J. Am. Ceram. Soc. 93 (2010) 1218–1220.
[12] J.B. Lim, S. Zhang, H.J. Lee, J-.H. Jeon, T.R. Shrout, Shear-mode piezoelectric properties of modified-$(K,Na)NbO_3$ ceramics for "Hard" lead-free materials, J. Am. Ceram. Soc. 93 (2010) 2519–2521.
[13] M. Ahtee, Structural phase transitions in sodium–potassium niobate solid solutions by neutron powder diffraction, Acta Crystallogr. A34 (1978) 309–317.
[14] D. Viehland, Y.H. Chen, Random-field model for ferroelectric domain dynamics and polarization reversal, J. Appl. Phys. 88 (2000) 6696–6707.
[15] R.E. Jeager, L. Egerton, Hot pressing of potassium–sodium niobates, J. Am. Ceram. Soc. 45 (1962) 209–213.
[16] S. Takahashi, Effects of impurity doping in lead zirconate–titanate ceramics, Ferroelectrics 41 (1982) 143–156.